RESEARCH PROGRESS IN MECHANICAL AND MANUFACTURING ENGINEERING
e-ISSN: 2773-4765

RPMME

Vol. 5 No. 1 (2024) 304-317
https://publisher.uthm.edu.my/periodicals/index.php/rpmme

Friction Stir Welding of Dissimilar Aluminium Alloys for Marine Applications

Nor Asyikin Mohd Yusof[1], Shazarel Shamsudin[1]*

[1] *1Faculty of Mechanical and Manufacturing Engineering, Universiti Tun Hussein Onn Malaysia, Parit Raja, 86400, Batu Pahat, Johor, MALAYSIA*

*Corresponding Author: shazarel@uthm.edu.my
DOI: https://doi.org/10.30880/rpmme.2024.05.01.036

Article Info

Received: 05 March 2024
Accepted: 15 June 2024
Available online: 15 September 2024

Keywords

Friction Stir Welding (FSW), Aluminum alloy AA6061 and AA5083, Surface Response Methodology (RSM), Design of experiment (DOE), Tensile strength, hardness and microhardness

Abstract

The FSW process utilises the aluminium alloys of AA6061-T6 and AA5083-H116 as workpieces. The size of the specimen is 65mm x 50mm x4mm and butt joint type is selected. The FSW parameters selected are material thickness (3 mm, 4 mm, and 5 mm), rotational speed (800 rpm, 1200 rpm, and 1600 rpm), feed rate/linear speed (30 mm/min, 60 mm/min, and 90 mm/min), pin length (92.5 %, 95% and 97.5% of material thickness) and dwell time (15 min, 20 min and 25 min). The optimization of the responses of tensile strength and hardness will be carried out through Response Surface Methodology (RSM) design. The tensile test is carried out using Universal Testing Machine. The microhardness underneath the sub-surface layer of the weld joint is measured by Vickers Hardness Tester. Linear speed and pressure required welding and types of tools. Samples friction stir welding were added depending on the application of design of experiment (DOE) method by means of (RSM) and use Minitab to get optimization of the tensile strength and linear relationship between the results and parameters.

1. Introduction

Welding is defined as "a joining process that produces coalescence of materials by heating them to the welding temperature, with or without the application of pressure or pressure alone, and with or without the use of filler metal." [1]. A weld is formed when separate pieces of material to be joined combine and form one piece when enough heat is applied to raise the temperature to a point where the pieces melt or soften and flow together, enough pressure is applied to cause the surface to coalesce, or enough heat and pressure are combined to cause the individual pieces of material to unite and form a single piece. A non-consumable rotating tool with a specially formed pin and shoulder is inserted into the opposing edges and rotated along the connection line while attaching sheets or plates. The tool has two basic functions such as heating the workpiece and material movement to generate the junction.

Many aluminum alloys from the 5xxx and 6xxx series have been developed to cater for such applications and are commonly used. Friction stir welding (FSW) is a process that produces joints with high strength and few flaws. realized by using optimum process parameters. have high strength and minimal defects. Designers are currently looking for new materials to lower ship weight due to the growing need for building larger ships. The researchers found a solution by applying aluminum alloys in marine structures due to their advantages of light weight, low corrosion, and high mechanical strength. Aluminum alloys from 5xxx series have been increasingly applied in the marine fabrication industries due to its unique mechanical and corrosion properties while 6xxx series also can be used in the atmosphere without any serious risk of corrosion as well.

The friction stir welding is selected because of its multiple advantages over other traditional welding methods. A comprehensive study should be carried out to understand from a practical viewpoint how process variables in FWS will influence the marine structure strength. The scope of this research includes the FSW process utilizes the aluminum of AA6061-T6 and AA5083-H116 as work pieces, size of the specimen is 65mm x 50mm x 4mm and butt joint type is selected, the FSW parameters selected are material thickness (3mm, 4mm, and 5mm), rotational speed (800 rpm, 1200 rpm, and 1600 rpm), feed rate/linear speed (30 mm/min, 60 mm/min, and 90 mm/min), pin length (92.5%, 95% and 97.5% of material thickness) and dwell time (15 min, 20 min and 25 min).

2. Materials and Methods

2.1 Material Preparation

The aluminum alloys AA6061-T6 and AA5083-H116 were chosen for this study for a variety of reasons, including their suitability for deep-sea structure applications, heat treatable alloys where strength can be tailored, and among common materials used in maritime due to their light weight, higher strength, and good machinability. Friction stir welding was chosen due to its numerous advantages over other traditional welding processes. A complete study should be conducted to determine how process variables in FWS will affect marine structure strength from a practical standpoint.
The steps for the FSW experiment technique are as follows:

1. Make raw AA6061 and AA5083 alloys with thicknesses of 3 mm, 4 mm, and 5 mm.
2. Inserting specimens into the table design.
3. Table 3.4 shows the design of experiment (DOE) are employed in friction stir welding. Figure 3 depicts a total of 19 samples. Six were welded with the help of a new design tool.
4. Using a CNC jet water, cut tensile test specimens.
5. Tensile strength samples are cut according to ASTM specifications. A CNC water jet is used to mark E8/E8M 15a cut samples.
6. Tensile strength testing was performed on the materials illustrated in Figure 3.8, and the tensile strength results from the new design tool and the standard design tool of friction stir welding were compared.

2.2 Design of Experiment (DOE)

In some circumstances, data must be generated, such as through a Design of Experiment (DOE), which is discussed later in this article. In this project, Minitab 21 was used to demonstrate graphical and statistical data analyses and DOE techniques. Minitab includes several statistical approaches. This will be addressed in separate parts for each statistical method under consideration. Experiments can be designed in a variety of ways to acquire this information. Therefore, a half factorial design with only one replicate and three centre points was chosen to execute the experiment. A total of nineteen runs were carried out according to the half factorial design with three centre points. The tensile strength of the welded material will be investigated based on input factors such as thickness, holding time, length, spindle speed and feed rate. The overall results of the experiments are presented in the table below.

Table 1 *Design of the process parameters*

Factor Symbol	Input Parameters (Factors)	Level		
		Low (-1)	Centre (0)	High (+1)
Th	Thickness (mm)	3	4	5
Tt	Holding Time (s)	15	20	25
L	Length (m)	0.1	0.2	0.3
SS	Spindle Speed (RPM)	800	1200	1600
Fr	Feed Rate (mm/min)	30	60	90

Table 2 *Experimental design using half factorial design*

Std Order	Run Order	Center Points	Blocks	Input Parameters (Factors)				
				Th	Tt	L	SS	Fr
1	1	1	1	3	15	0.3	800	90
2	2	1	1	5	15	0.3	800	30
3	3	1	1	3	25	0.3	800	30
4	4	1	1	5	25	0.3	800	90
5	5	1	1	3	15	0.1	800	30
6	6	1	1	5	15	0.1	800	90
7	7	1	1	3	25	0.1	800	90
8	8	1	1	5	25	0.1	800	30
9	9	1	1	3	15	0.3	1600	30
10	10	1	1	5	15	0.3	1600	90

2.3 Test and Inspection

2.3.1 Tensile Strength

The tensile test is carried out using Universal Testing Machine. The microhardness underneath the sub-surface layer of the weld joint is measured by Vickers Hardness Tester. Tensile test specimens prepared in accordance with ASTM E8 standards will be milled or wire-cut. The tensile test machine's capacity is ten tons, and the jaws' speed will be set at three millimeters per minute. The tension instances are shown. According to the ASTM E04-08 standard for flat samples, tensile samples are made using conventional machining. To ensure that the welding zones stayed in the center of the tensile dog-bone sample, samples are initially oriented perpendicular to the welding direction or rolling direction. The APEX T20000 machine is used for the tensile testing described in the following sections. A 2”-gauge digital extensometer positioned around the center of the weld sample under test is used to measure the elongation. The ASTM E08-08 standard for flat samples in tension is used for all testing. Tensile ultimate strength is taken as the greatest value and measurements for yield strength are done at 2% offset yield. Without applying heat, a tensile test is conducted.

2.3.2 Microhardness Testing

The microhardness underneath the sub-surface layer of the weld joint is measured by Vickers Hardness Tester. Center line hardness profiles are taken for each sample using a Clark CM- 100AT manual micro-hardness tester equipped with a Vickers’s indenter. Vickers Hardness Tester was performed on disk cross section along the mid-plane, with post consolidation heat treated conditions. On each disk cross section, a hardness traverse was made along an entire diameter with an indentation spacing. Clemex digital camera and software were used to take the hardness readings at x500 magnification. The readings were taken from a clear focused optical image. All indents were performed at 300gf loading and at least 250μm apart as to ensure x3 diagonal spacing between indents as per ASTM E384 standard.

2.3.3 Density Test

A density test is a sort of material test that can be performed in the field or in a lab to ascertain the density of compacted soil, rock, or other materials. Density is a physical characteristic of matter and is also known as the mass per unit volume of a substance. A variety of methods are available for density testing. To assess how much dirt, sand, or other fine material can fit in a specific area with the current amount of compaction, one conventional method involves taking a core sample in a tube and weighing the sample. The materials can be weighed both dry and wet to provide further density data. Other material tests, such as an analysis to identify the types of materials in the sample, can also be carried out in laboratories. Without altering the substance's chemical makeup, a physical attribute can be measured. Since pure substances have distinct densities, determining a substance's density can aid in identifying it. Density chips describe the densities of several types of aluminum.

2.3.4 Optical Microstructure

On specimens that have undergone the etching procedure, this equipment is used. An optical microscope (OM) is a measurement device, and it is used to investigate microstructure studies, including grain size (OM). In material research involving problem-solving, failure analysis, the creation of innovative materials, and quality control, an optical microscope is a useful instrument. For many years, fiber reinforced composites' micro and microstructure have been studied using microscopy. The Olympus microscope can be imagined using both reflection and transmission. The optical microscope will be utilized in this study.

2.3.5 Microstructure (SEM)

By scanning the surface of the sample with a focused beam of electrons, scanning electron microscopy (SEM) creates an image of the sample surface. Layer-by-layer growth can be seen in various phases in SEM photos. Based on the photos, the step propagation velocity may be calculated. To find any weld faults that may be present and to examine the microstructure of the weld-affected zone, microstructural (SEM) examinations of the samples' welds will be performed. To examine the microstructure of a material, microstructural examinations can be carried out using a variety of microscopy techniques. After that, all samples go through mounting, grinding, polishing, and etching procedures that will be covered.

3. Results and Discussion

3.1 Surface Quality on Welded Area

Table 3 *Visual inspection on the welded area of specimens in preliminary experiments with high tensile strength*

Specimen No.	Remarks	The appearance of joint after welding.
1	To improve the welding condition, tool and fixture, samples are rewelding with the same variables. The weld has a rough aspect.	
2	The appearance of joint welding is good and consistent. The ends just require repair	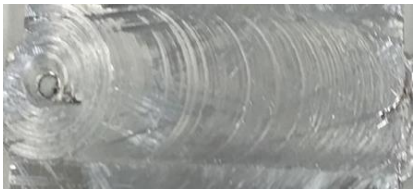
3	The appearance of joint welding is satisfactory. The weld ends will be taken out.	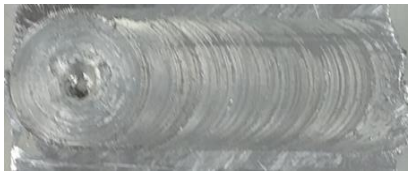
4	Re-weld the sample with the same variables. The weld looks nice, and the tool's left shoulder does not touch the workpiece.	
5	The beginning and end of the joint will be eliminated.	

6	A minor crack at the weld's end will be repaired.	
7	The appearance of the weld is good, but there is a minor crack near the end of the weld.	
8	The appearance of the weld is good, and the welding is regular.	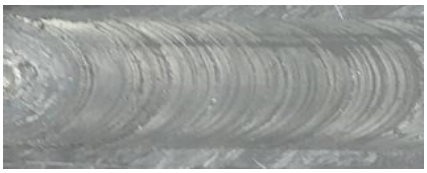
9	Reweld the sample. The weld appears to be good, with a lock of fusion at the end of the joint weld.	

Table 4 *Initial attempt is made based on visual assessment of the welded area of specimens with low tensile strength*

Specimen No.	Remarks	The appearance of joint after welding.
1	Lack of plastic deformation on the left side of the welding line because of not touching the side of the soldering piece	
4	There is a minor crack at the end of the weld. The beginning and end of joint welding will be eliminated.	
8	The appearance of the weld is good.	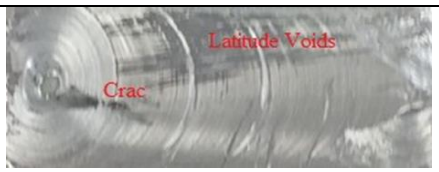
9	A good welding smoothness is achieved when the tool's right shoulder does not meet the workpiece.	

3.2 Result and Discussion of RSM Analysis

19 run experiments were conducted by giving the input parameters varied of input parameters. The output parameters selected for the experiment are Ultimate Tensile Strength (UTS). A blend of aluminium alloys AA5083 and AA5061 was used in the experiment. The UTS of the friction stir-welded seam was predicted using an ensemble machine learning model with FSW parameters as input components and the UTS as a response variable. The results are shown in table below.

Table 5 *Tensile strength result of samples*

Std Order	Run Order	Center Points	Blocks	Input Parameters (Factors)					Response
				Th	Tt	L	SS	Fr	TS (MPa)
1	1	1	1	3	15	0.3	800	90	209.70
2	2	1	1	5	15	0.3	800	30	146.91
3	3	1	1	3	25	0.3	800	30	227.46
4	4	1	1	5	25	0.3	800	90	285.58
5	5	1	1	3	15	0.1	800	30	146.91
6	6	1	1	5	15	0.1	800	90	164.56
7	7	1	1	3	25	0.1	800	90	279.65
8	8	1	1	5	25	0.1	800	30	237.89
9	9	1	1	3	15	0.3	1600	30	195.18
10	10	1	1	5	15	0.3	1600	90	146.91
11	11	1	1	3	25	0.3	1600	90	282.61
12	12	1	1	5	25	0.3	1600	30	227.46
13	13	1	1	3	15	0.1	1600	90	155.29
14	14	1	1	5	15	0.1	1600	30	156.39
15	15	1	1	3	25	0.1	1600	30	282.61
16	16	1	1	5	25	0.1	1600	90	211.64
17	17	0	1	4	20	0.2	1200	60	201.53
18	18	0	1	4	20	0.2	1200	60	209.70
19	19	0	1	4	20	0.2	1200	60	195.18

Table 6 *Tensile strength result of samples using normal and new design tool*

No.	Input Parameters (Factors)					Response	
	Th	Tt	L	SS	Fr	TS using normal design tool (MPa)	TS using new design tool (MPa)
1	3	15	0.3	800	90	209.70	280
2	5	15	0.3	800	30	146.91	196
3	3	25	0.3	800	30	227.46	250
4	5	25	0.3	800	90	285.58	285
5	3	15	0.1	800	30	146.91	153
6	5	15	0.1	800	90	164.56	190
7	3	25	0.1	800	90	279.65	290
8	5	25	0.1	800	30	237.89	278
9	3	15	0.3	1600	30	195.18	220
10	5	15	0.3	1600	90	146.91	197
11	3	25	0.3	1600	90	282.61	285
12	5	25	0.3	1600	30	227.46	270
13	3	15	0.1	1600	90	155.29	205
14	5	15	0.1	1600	30	156.39	215
15	3	25	0.1	1600	30	282.61	317
16	5	25	0.1	1600	90	211.64	250
17	4	20	0.2	1200	60	201.53	245
18	4	20	0.2	1200	60	209.70	240
19	4	20	0.2	1200	60	195.18	245

Table 7 *Rate improvement percentage tensile strength by using normal and new design tool of FSW*

No.	TS using normal design tool (MPa)	TS using new design tool (MPa)	Improvement (%)	Notes
1	209.70	280	33.53	Increase rate
2	146.91	196	25.05	Increase rate
3	227.46	250	9.91	Increase rate
4	285.58	285	-0.20	Decrease rate
5	146.91	153	4.15	Increase rate
6	164.56	190	15.46	Increase rate
7	279.65	290	3.71	Increase rate
8	237.89	278	16.86	Increase rate
9	195.18	220	12.72	Increase rate
10	146.91	197	34.10	Increase rate
11	282.61	285	0.85	Increase rate
12	227.46	270	18.70	Increase rate
13	155.29	205	32.01	Increase rate
14	156.39	215	37.48	Increase rate
15	282.61	317	12.17	Increase rate
16	211.64	250	18.13	Increase rate
17	201.53	245	21.57	Increase rate
18	209.70	240	14.45	Increase rate
19	195.18	245	25.53	Increase rate

Table 8 shows the findings of the UTS quadratic model analysis. According to the results of the investigation, the quadratic model is statistically significant for tensile strength response except for the spindle speed (SS), 2-Way Interaction, and Tt*Fr components. The quadratic model is statistically significant because the P-value for the other terms is less than 0.05. The model terms sheet thickness (Th), holding time (Tt), tool pin length (L), and feed rate (Fr) all have a major impact on the tensile strength reaction. Furthermore, the interaction between parameters such as Th*SS and L*Fr influences the response, as indicated by p-values. The coefficient of determination R^2value is 0.9947, suggesting that the model explained about 99.47% of the total variation and that only roughly 0.53% was not explained. The high percentage of R^2 shows that the regression model explains the connection between the independent factors and the dependent variable (response) very well. As shown in Table 9 the predicted R^2 of 0.9947 indicates that the model's error was just 2.11% between the projected and actual test.

Table 8 *Coded Coefficient*

Term	Effect	Coef	SE Coef	T-Value	P-Value	VIF
Constant		209.77	1.43	147.04	0.000	
Th	-25.20	-12.60	1.43	-8.83	0.000	1.00
Tt	89.08	44.54	1.43	31.22	0.000	1.00
L	10.92	5.46	1.43	3.83	0.006	1.00
SS	-5.13	-2.56	1.43	-1.80	0.115	1.00
Fr	14.45	7.22	1.43	5.06	0.001	1.00
Th*SS	-18.01	-9.00	1.43	-6.31	0.000	1.00
Tt*L	-7.97	-3.99	1.43	-2.79	0.027	1.00
Tt*Fr	6.68	3.34	1.43	2.34	0.052	1.00
L*Fr	17.50	8.75	1.43	6.13	0.000	1.00
SS*Fr	-30.63	-15.32	1.43	-10.74	0.000	1.00
Ct Pt	-	-7.63	3.59	-2.13	0.071	1.00

Table 9 *ANOVA results of tensile strength by Minitab 21*

Source	DF	Adj SS	Adj MS	F-Value	P-Value	
Model	11	42550.1	3868.2	118.79	0.000	Significant
Linear	5	35694.7	7138.9	219.24	0.000	Significant
Th	1	2540.7	2540.7	78.03	0.000	Significant
Tt	1	31737.4	31737.4	974.67	0.000	Significant
L	1	476.5	476.5	14.64	0.006	Significant

SS	1	105.2	105.2	3.23	0.115	
Fr	1	834.9	834.9	25.64	0.001	Significant
2-Way Interactions	5	6708.2	1341.6	41.20	0.000	
Th*SS	1	1297.1	1297.1	39.83	0.000	
Tt*L	1	254.2	254.2	7.81	0.027	
Tt*Fr	1	178.5	178.5	5.48	0.052	
L*Fr	1	1225.0	1225.0	37.62	0.000	
SS*Fr	1	3753.4	3753.4	115.27	0.000	
Curvature	1	147.2	147.2	4.52	0.071	
Error	7	227.9	32.6	-	-	
Lack-of-Fit	5	122.0	24.4	0.46	0.791	Insignificant
Pure Error	2	106.0	53.0	-	-	
Total	18	42778.0	-	-	-	

Pareto chart in Figure 1 below shows of standardize effects demonstrates that factor B (holding time, Tt) is the most influential element on the response, followed by factor DE, the interaction between spindle speed (SS) and feed rate (Fr). However, the thickness (Th) of the aluminium sheet, as well as the relationship between tool pin length and feed rate, have a considerable impact on tensile strength (TS). The length (L) of the elements that passed the reference red line determines their significance. Other factors that do not exceed the reference line are unimportant. To improve the model, these inconsequential elements can be deleted using a backward elimination process.

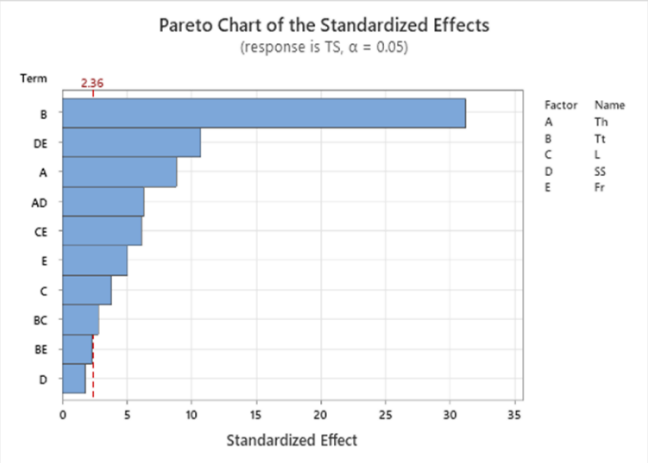

Fig. 1 *Pareto chart of the standardized effects*

For each value, a residual is computed. Each residual is the difference between a value entered and the mean of all values in that group. Residual plots for tensile strength in Figure 2 depict a normal probability map of tensile strength's residuals. The fact that the residual is so near to the straight line indicates that the error is minor and normally distributed. Hence random scatter for residents versus fits response. The random dispersion of points has a constant variance and an even distribution. Similarly, the dispersed points imply that the model meets the DOE projection. Meanwhile, suggesting that the model meets the analysis of variance prediction. The regression model fits reasonably well with the observed values.

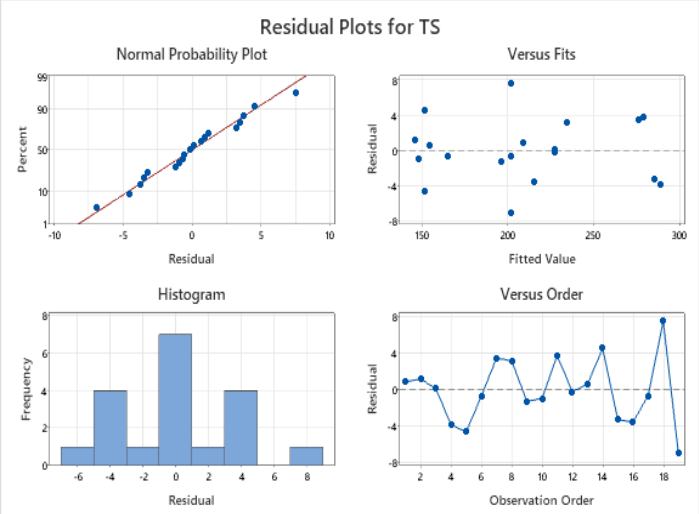

Fig. 2 *Residual plots for tensile strength*

The prediction of tensile strength for the developed material can be obtained by regression equation in uncoded units generated by ANOVA in equation below.

TS = -105.8 + 14.41 Th + 9.166 Tt + 39.0 L + 0.1602 SS + 0.744 Fr - 0.02251 Th*SS - 7.97 Tt*L
+ 0.02227 Tt*Fr + 2.917 L*Fr - 0.001276 SS*Fr - 7.63 Ct Pt

The TS is linearly dependent on the holding time Tt factor, as shown by the main effect graphs in Figures 3 and 4. The TS decreases as the thickness of the aluminium sheet component increases. The tool pin length and feed rate factor have a favourable effect on TS responsiveness. Furthermore, low spindle speed has a greater affect than high spindle speed.

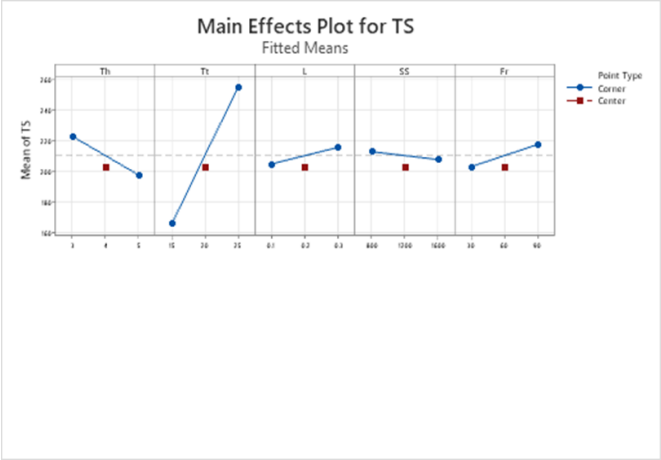

Fig. 3 *Main effects plots for tensile strength*

Research Progress in Mechanical and Manufacturing Engineering Vol. 5 No. 1 (2024) p. 304-317

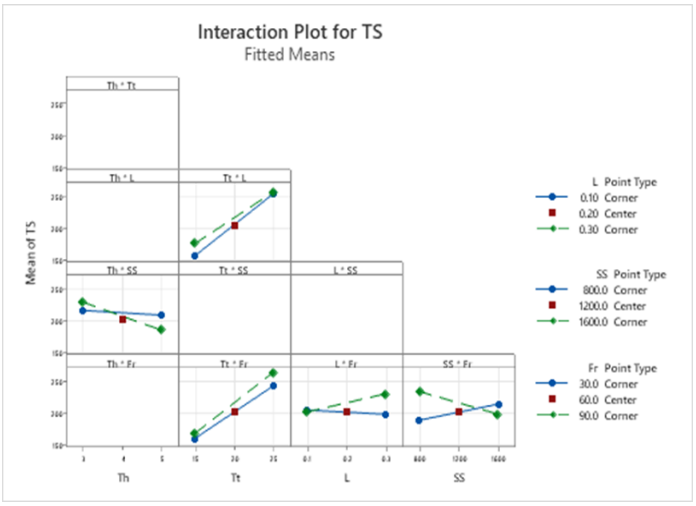

Fig. 4 *Interaction plots for tensile strength*

3.3 Response Optimization for Tensile Strength

Response optimization assists you in identifying the collection of variable settings that jointly optimize a single response or a set of responses. The response optimizer method is used to demonstrate which factors affect the welded product individually and how they affect the response variable (tensile strength). This procedure produced the highest tensile strength value. Figure 5 depicts an examination of the design of experiment (DOE) optimizer response for tensile strength. According to the results in Figure 5, the higher feed rate (F.R) and deeper pin (D.P) values are the model's optimum values. To attain maximum tensile strength qualities, the RSM was used to optimize the input parameters. Figure 4.6 shows the ideal parameter values that can result in a maximum tensile strength of 220.12 MPa.

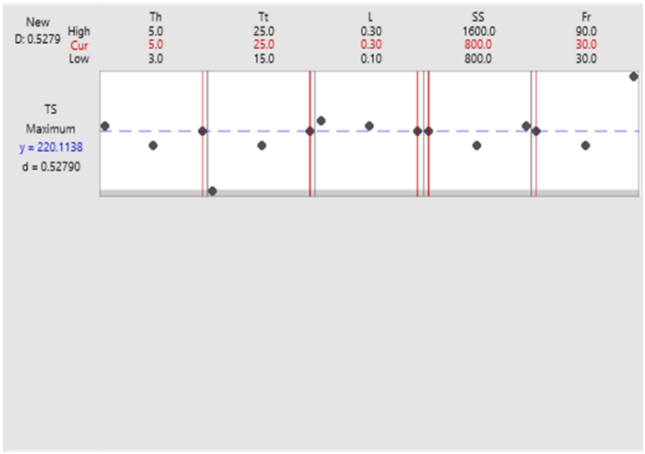

Fig. 5 *Optimization plot for tensile strength*

3.4 Results of Microhardness Test

Table 10 shows the microhardness values based on the DOE input parameters thickness (mm), spindle speed (rpm), and feed rate (mm/min). The microhardness on all specimens tested is within the permitted range. Furthermore, as shown in Table 4.11, increasing the thickness and feed rate reduces the microhardness at a fixed spindle speed of 800 rpm. It is mostly due to the shorter exposure period to the welding zone, which results in less plasticity in that region. The optimum microhardness value (125.72 HVO-1) resulted in higher values of thickness (5 mm) and feed rate (90 mm/min) at constant spindle speed (1200 rpm). It can also be seen that increasing the spindle speed above 1200 rpm reduces the microhardness value.

Table 10 *Microhardness values*

Workpiece No.	Input Parameters (Factors)			Microhardness (HV0.1)
	Thickness (mm)	Spindle Speed (rpm)	Feed Rate (mm/min)	
1	3	800	30	110.830
2	4	800	60	90.784
3	5	800	90	61.126
4	3	1200	30	90.784
5	4	1200	60	91.117
6	5	1200	90	125.723
7	3	1600	30	105.891
8	4	1600	60	103.152
9	5	1600	90	91.989

3.5 Microstructure Examination by OM

Figure 6 clearly shows the line of friction stir welding in the welding region of two different alloys. Also, the stitch weld shows a clear and homogenous and some dendritic line cracks appear around the weld region. However, it is regarded as the best weld due to the lack of welding faults and the variable parameters that provided enough heat to weld. The microstructure of all three specimens through optical microstructure analysis (specimens No.3, 5 and 7) revealed that the specimen No.7 has the deprived microstructure and most of the metals melted and causing poor microstructure which leads to achieve lower amount of tensile strength and hardness of the weld joint. This is because of the increased heat generated in the weld zone. However, the microstructure of specimen No. 5 shown in Figure 7 exhibits minor voids and line cracks in the weld zone. Finally, Figure 6 depicts the microstructure of specimen No. 3, which has a better microstructure and the highest tensile strength value.

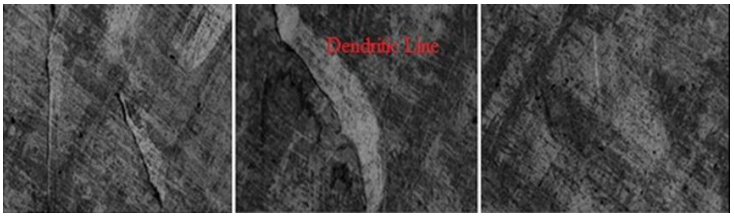

Fig. 6 *Optical microstructure for specimens with highest values of tensile strength (Specimen No. 3)*

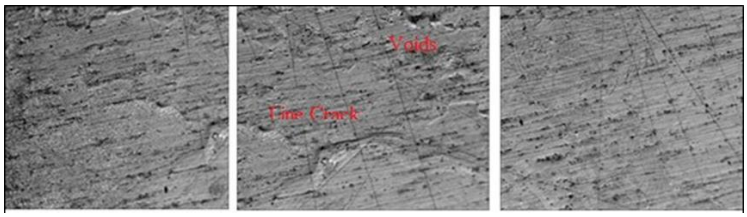

Fig. 7 *Optical microstructure for specimens with medium values of tensile strength (Specimen No. 5)*

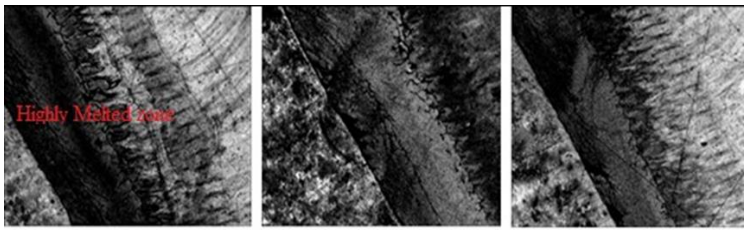

Fig. 8 *Optical microstructure for specimens with lowest values of tensile strength (Specimen No. 7)*

3.6 3.6 Analysis of Microstructure by SEM

The microstructure of weld joint for specimen No. 3 is shown in Figure 9. Both alloys were properly welded, with no cracks but heterogeneous granules in the weld zone. These heterogeneous granules generate

inadequacy in the weld region and can lower mechanical characteristics. However, the initial parameters of friction stir welding can be adjusted to provide the optimal mechanical properties. Figure 10 shows the microstructure of specimen No. 5. Some dendritic fractures (line cracks) formed at the heat affected zone (HAZ) in the weld region. Figure 11 shows the microstructure (SEM) of specimen No.7. The microstructure shows voids on account of higher amount of heat generated in the weld region due to higher rotational speed. Such voids result in a poor microstructure of the weld joint, resulting in a reduced tensile strength value. All these defects have a reduction in the tensile strength result because of the high speed of rpm.

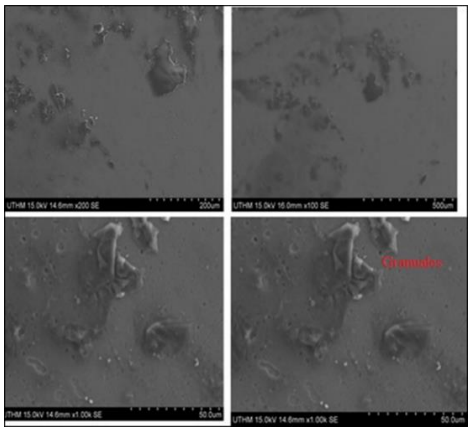

Fig. 9 SEM for specimen no. 3

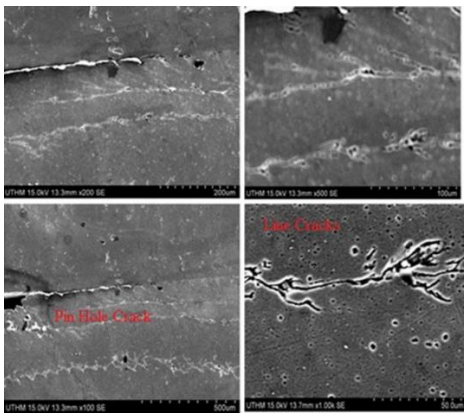

Fig. 10 *SEM for specimen no. 5*

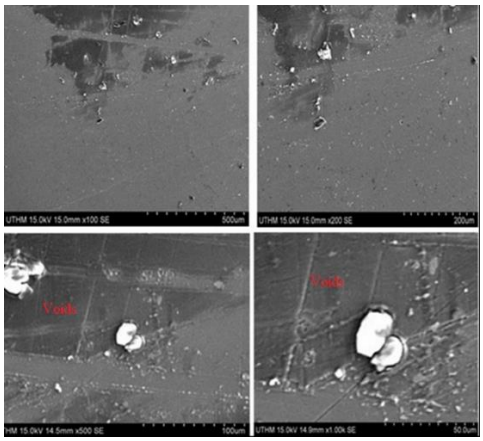

Fig. 11 *SEM for specimen no. 7*

3.7 3.7 Results of Density Test

The buoyant force is equal to the difference between the weight of an object immersed in a fluid Wi and the weight of the object outside in air Wo. Changing the input process parameters changed the physical qualities of the welding produced by the FSW process. All the values recorded and listed in Table 4.12 were based on an

average of three observations taken at room temperature. As-received density for AA6061 is 2.7 g/cm^3 and 2.67 g/cm^3 for AA5083. All the measured density values for all specimens are very close to the base material, demonstrating that all specimens were properly fabricated using the FSW process. The density values for all specimens are within acceptable limits.

Table 11 *Results of density of distilled of specimens*

No.	Temperature (°C)	Weight in air (g)	Weight in liquid (g)	Density (g/cm^3)
1	27.3	1.5127	0.5867	2.65
2	27.7	2.4375	0.9214	2.66
3	27.4	2.1049	0.7949	2.63
4	27.5	1.7192	0.6489	2.63
5	27.5	2.4966	0.9558	2.60
6	27.5	2.7439	1.0176	2.68
7	27.6	2.2702	0.8477	2.66
8	27.6	2.4267	0.9110	2.65
9	27.7	2.9563	1.1055	2.66

4. Conclusions

The current study's findings such as the maximum value of tensile strength using normal design tool are 285.58 MPa achieved for specimen No.4 at higher values of feed rate 90 mm/min and length of 0.3 mm, while the maximum value of tensile strength using new design tool are 290 MPa achieved for specimen No. 7 at higher values of feed rate 90 mm/min and length of 0.1 mm. Next, we can see the lowest value of tensile strength using normal design tool are 146.91 MPa with an influence of 800 rpm of tool speed, 30 mm/min of feed rate and length of 0.3 m achieved for specimen No.2, 5 and 10. Then, increasing the feed rate and length, the tensile strength increased for lower rotational speed of the spindle speed. According to the Minitab 21 simulation, F.R is the sole efficient parameter for forecasting and attaining the best response (tensile strength). The microstructure of the weld joint was examined using three specimens: the highest, medium, and lowest tensile strength values. The OM and SEM examination demonstrate that specimen No.3 is defect-free and contributes high tensile strength. The numerical model used in ANOVA to forecast the best values for constructing the specimens with FSW is effective.

As a result, the following future recommendations are made for furthering research into the FSW process. First, do more research into friction stir welding for various parts in many industrial applications such as welding pipe to pipe, lap welding, and welding similar and dissimilar materials. Next, it is suggested that the input parameters utilized in this study be altered to further analyze the mechanical, microstructure, and physical properties of the base metals employed in this study. After that, it is suggested that temperature be employed as an input parameter for the FSW process to investigate its effect on the mechanical, microstructure, and physical properties of the base metals used in this study. Lastly, new types of tool profiles are suggested to further investigate the research on the basic metals employed in this study and it is suggested that the fatigue and corrosion properties of similar and dissimilar metals be examined for the FSW process.

Acknowledgement

The authors wish to thank to the Faculty of Mechanical and Manufacturing Engineering, Universiti Tun Hussein Onn Malaysia that has supported on the accomplishment of research activity.

References

[1] Elangovan K, Balasubramanian V. Effect of pin profile and rotational speed of the tool on the formation of friction stir processing zone in AA6061 aluminium alloy. J Mater Manuf Processes, in press.
[2] W.M. Thomas, E.D. Nicholas, J.C. Needham, M.G. Murch, P. Templesmith, C.J. Dawes, G.B. Patent Application No. 9125978.8 (December 1991).
[3] C. Dawes, W. Thomas, TWI Bulletin 6, November/December 1995, p. 124.
[4] B. London, M. Mahoney, B. Bingel, M. Calabrese, D. Waldron Proceedings of the Third International Symposium on Friction Stir Welding, Kobe, Japan, 27–28 September (2001)
[5] C.G. Rhodes, M.W. Mahoney, W.H. Bingel, R.A. Spurling, C.C. Bampton Scripta Mater., 36 (1997), p. 69
[6] G. Liu, L.E. Murr, C.S. Niou, J.C. McClure, F.R. Vega Scripta Mater., 37 (1997), p. 355
[7] K.V. Jata, S.L. Semiatin Scripta Mater., 43 (2000), p. 743

[8] S. Benavides, Y. Li, L.E. Murr, D. Brown, J.C. McClure Scripta Mater., 41 (1999), p. 809
[9] L.E. Murr, Y. Li, R.D. Flores, E.A. Trillo Mater. Res. Innovat., 2 (1998), p. 150
[10] Y. Li, E.A. Trillo, L.E. Murr J. Mater. Sci. Lett., 19 (2000), p. 1047
[11] Y. Li, L.E. Murr, J.C. McClure Mater. Sci. Eng. A, 271 (1999), p. 213
[12] H.B. Cary, Modern Welding Technology, Prentice-Hall, New Jersey, 2002.
[13] C.J. Dawes, W.M. Thomas Weld. J., 75 (1996), p. 41
[14] A Concise Anglo-Saxon Dictionary by John R. Clark Hall, Herbert T. Merritt, Herbert Dean Meritt, Medieval Academy of A, merica -- Cambridge University Press 1960 Page 289
[15] K. Weman, "Introduction to welding," Weld. Process. Handb., pp. 1–12, 2012
[16] R. Akeret Extrusion of semifinished products in aluminum alloys, M. Bauser, G. Sauer, K. Siegert (Eds.), Extrusion (2nd ed.), ASM International, Materials Park, OH 44073-0002 (2006), pp. 207-226
[17] Mishra RS, Ma ZY. Friction stir welding and processing. Mater Sci Eng R: Rep 2005;50:1–78
[18] Mahoney, M.W., Rhodes, C.G., Flintoff, J.G., Spurling RA., Bingel WH. 1998. Properties of friction stir welded 7075 T651 aluminium. Metal Mater Trans A 1998;29:1955–64.
[19] Colligan, K., 1999.Material flow behaviour during friction stir welding of aluminium. Weld J;7pp.229–37.
[20] Pashazadeh H, Masoumi A, Teimournezhad J. Numerical modelling for the hardness evaluation of friction stir welded copper metals. Mater Des 2013;49:913–21
[21] He X. Numerical studies on friction stir welding of lightweight materials. Adv Mater Res 2013;743:118–22.
[22] Archimedes.(n.d.). http://www.appstate.edu/~cockmanje/labs/1103/spring/archimedes#:~:text=Archimedes%EF%BF%BD%20Principle%3A&text=We%20can%20determine%20the%20density,forces%20equals%20the%20buoyant%20force.